



Development of material property for the side body structure of a passenger car

Beruk Hailu and T. Ashok Kumar*

Department of Mechanical Engineering, Institute of Technology, Haramya University, P.O Box 138, Dire Dawa, Ethiopia
ntashoknt.1966@gmail.com

Available online at: www.isca.in, www.isca.me

Received 20th April 2018, revised 4th June 2018, accepted 14th June 2018

Abstract

Car safety becomes an issue almost immediately after the invention of the automobile. To protect occupants from a direct impact, the passenger compartment and the structure of the vehicle should keep its shape in a crash. Side-impact collisions are the most critical crash scenarios and a second leading cause of death and injury of people in the traffic accidents across the world. Car's side body structures like side impact beams of doors and double skin pillars were developed to reduce the impact and depth of side body structures deformation into the passenger compartment in side impact crashes. Assessing the effectiveness of side impact beams are significant for reducing occupant fatalities and serious injuries. By using the relation between maximum absorbed impact energy and minimum structural weight the new techniques was developed and also crashworthiness performance was improved related with material optimization and thickness.

Keywords: Crashworthiness, optimization, body structures, finite element analysis.

Introduction

Car accidents occur in a random manner. An automobile can be impacted from any direction at different speeds. It can also include an automobile impacting another automobile, which in turn can be the same or different from the first automobile. This shows how automobiles affect and being affected by each other in crash situations¹. Crash pulse is the deceleration induced by impact on the human body. Head injury criterion is used to measure the damage from crash pulse on the brain, and it should be less than a certain limit by regulations².

Prior to the accident, the vehicle, the occupant and their organs are all travelling at the same speed. However, because they are not rigidly attached to each other, they move independently when large G-forces are applied³. Plastics and composites are widely used to make body panels, bumper systems, flexible components, trims, drive shaft and transport parts of cars. In the field of rotor manufacturing for the purpose of easy machining metal was replaced with Resin Transfer Mouldings (RTM)⁴. In manufacturing harmonic devices composites are used as flexible materials⁵.

When considering the safety benefits arising from using composite materials in structural components of a vehicle, two material-related safety benefits may be identified: improvements in Specific Energy Absorption (SEA) and added resistance to intrusion. The most commonly presented safety benefit of using composites in vehicle structural components is the possibility of higher SEA than available with metallic materials such as steel and aluminium. In metallic structures, energy is absorbed through plastic deformation as the structure is folded in an

accordion manner. In contrast, the mechanism by which composite materials absorb energy most efficiently is through material fragmentation, such that the composite material disintegrates along a crush front as crushing progresses. Specific Energy of Different Materials is given in Figure-1. The energy absorption capability⁶⁻⁸ of the composite structure mainly depends on the:

Fiber Material: Physical properties of the fiber material directly influences the specific energy absorption of the composite. The brittle nature of the fiber results in more energy absorption rather than the ductile nature of the fiber, which fails by progressive folding.

Matrix Material: Specific energy absorption linearly increases with the matrix compressive strength.

Fiber and Matrix Combination: Due to crushing by high energy fragmentation, matrix material with a higher failure strain has high energy absorption than the fiber material.

Fiber Orientation and Lay-up: High energy absorption composites consist of layers of specified orientation and sequence plies.

Thornton et al.⁹ report that specific energy absorption is a linear function of the tensile strength and tensile modulus of the matrix resin, and that it increases with the order phenolic < polyester < epoxy for glass fiber tubes. Thornton et al.¹⁰ piloted a study examining the geometrical effects in energy absorption of circular, square, and rectangular cross section tubes. They determined that for a given fiber layup and tube geometry, the

specific energy follow the order, circular>square>rectangle. The result of the geometry and the strain distribution was examined using finite element analysis.

The results revealed that the critical strains were ominously push by the joint geometry. This exhibited that specific defects led to large fluctuations in the strains in the structure 5. Most work on the competitiveness of polymer composite technology came out in the early- to mid-1990s through the Partnership for a New Generation of Vehicles (PNGV). It is conventional wisdom within the industry that the use of polymer matrix composites in automobile structures cannot be defended on an economic basis. A 1995 study by IBIS Associates and the Rocky Mountain Institute, based on GM's ultra light BIW concept car, argued that concerns over economic viability may be misplaced. A 1999 study by the Rocky Mountain Institute has suggested that polymer composite BIW alternatives may be well suited to plat forming goals by providing a cheaper and more easily contoured solution for the customized elements not part of the shared platform. Erzen et al.⁴ designed side intrusion beam and analyzed it by finite element techniques. The initial ply failure found in the composite beam by applying the criteria of maximum stress failure then compared with steel beam by applying von Misses yield criteria. Simulation report revealed that the optimized Twintex beam start to fail close to 60mm related to a yield translation of 84mm for the allusion steel

beam. Since the study is imperfect in terms of full authentication of either the perception or modelling procedure. The work presented in this paper is to develop an effective and practical methodology for design optimization of vehicle structures for crashworthiness improvement for the passenger car.

Materials and methods

Development of material property for the side body structure: Material property development depends up on the required properties that particular structure to full fill. The structures that the study focuses on are: car side body structure of 4-door cars anti intrusion beams of door. Crashing load distributing on side-body structure is shown in Figure-2. Every material cannot be a right choice for a given application; hence, a suitable material selection must be made. Depending upon material selection, the design, processing, cost, quality, and performance of a product may vary. Advanced composites consist of either continuous or discontinuous fibers embedded in a matrix. Common fibers are glass, aramid, and carbon. Glass fibers are used extensively in commercial applications due to good balance of properties at low cost. Aramid fibers, being organic, have low densities and outstanding toughness. Carbon fibers have best combination of strength and stiffness but expensive among the three common fibers.

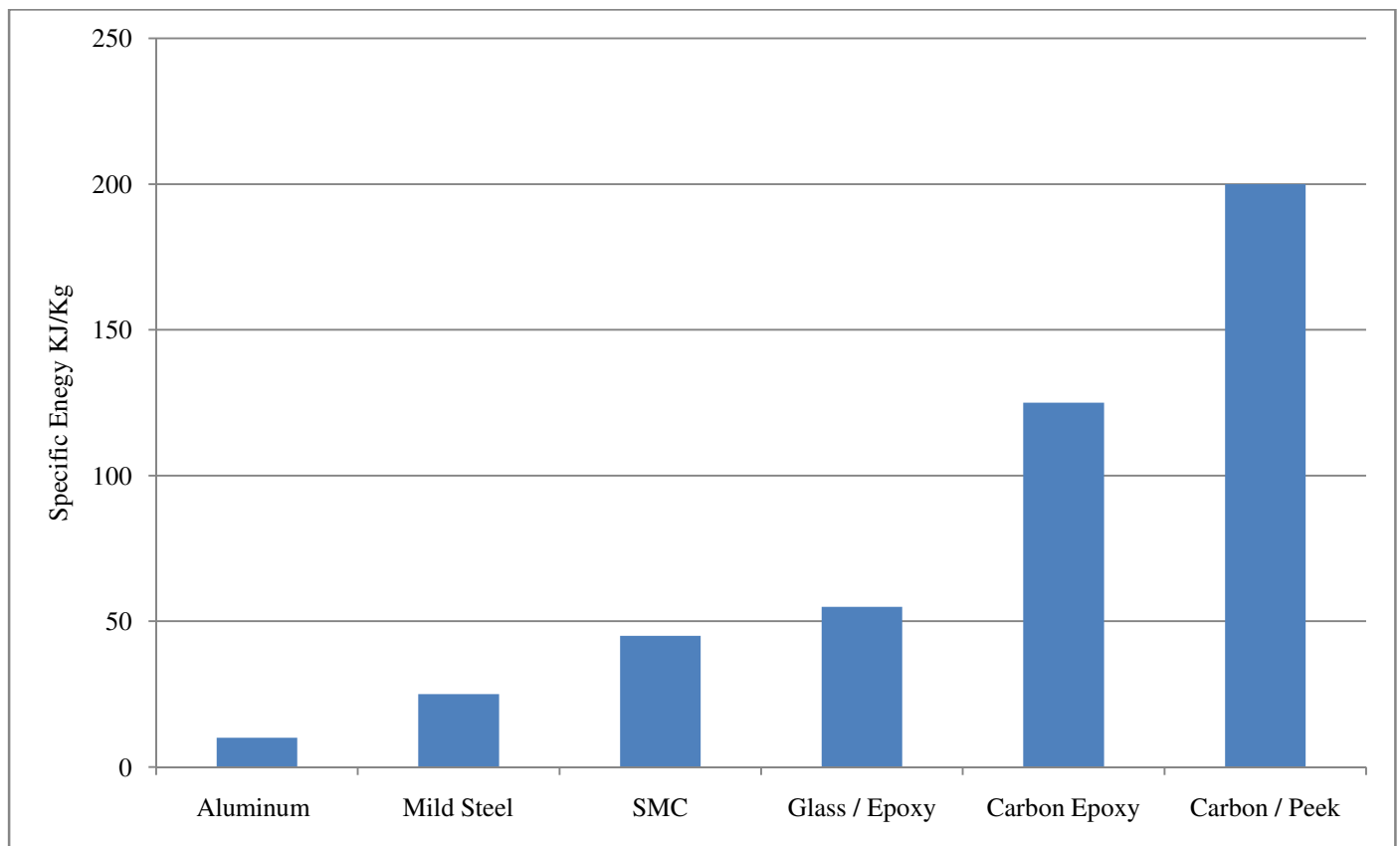


Figure-1: Specific energy of different materials¹¹.



Figure-2: Crashing load distributing on side-body structure¹².

Selection criteria for the composite that can substitute steel car side body structures are as follows: i. Light weight, ii. Impact resistance, iii. Advanced stiffness with strength, iv. Maximum strength, v. Minimal deformation, vi. High energy absorption capacity, vii. Affordable cost, viii. Corrosion resistance.

From the list five specific criteria were selected. The materials were determined and compared in properties systematically. Accordingly the total number of possible decisions, N_d , is given by: $N_d = 2^n - 1$, where n is the number of properties under consideration. In this design for five properties, N_d is calculated as: $N_d = 2^5 - 1 = 31$, we have ten number of decisions. Weighting factor is given in terms of property importance: i. Specific weight (g/cm^3), ii. High Strength, iii. Specific strength, iv. Cost, v. Specific energy absorption (KJ/Kg).

Comparison parameters on properties of fiber with fiber volume $V_f = 60\%$ is listed in Table-1.

Table-1: Comparison parameters on properties of fiber with fiber volume $V_f = 60\%$ ¹³.

Factors	Specific weight (g/cm^3)	Strength (MPa)	Specific strength	Specific Energy absorption (KJ/Kg)	Cost
Weight	1.5	3.5	2	2	1
Weighting factor	0.15	0.35	0.2	0.2	0.1

The composite materials, which are selected for comparison with respect to functional requirements of car side body structures, were: i. carbon /epoxy ($V_f 60\%$) = 87.2, ii. E-Glass/Epoxy ($V_f 60\%$) = 63.65, iii. Kevlar (Aramid) / Epoxy $V_f 60\% = 60.55$. The carbon /epoxy ($V_f 60\%$) is selected because of high merit rating of 87.2 ranks.

Analysis of laminate using Autodesk Simulation Composite Design:

In the Stress-Strain and Strength analysis the Autodesk simulation composite design simulated Global/Local Stress/Strain, Mid-Plane Strains/Curvatures, First Ply Failure and Progressive Failure value of IM-Carbon/Epoxy laminate.

New Lamina Properties based on Micromechanics:

The micromechanical finite element model utilizes the properties of fiber and matrix materials specified by the user, in addition to the fiber volume fraction specified by the user. Simulation Composite Design determines the composite material's elastic properties (e.g., moduli and Poisson ratios) by using the micromechanical finite element model to simulate the various fundamental load/deformation relationships of the composite material.

Laminate Thickness and Number of Lamina:

Laminate is a sheet construction made by stacking layers (plies or laminas) in a specified sequence. Based on the thickness of existing steel car side impact anti-intrusion beam which is about 2.00 mm to resist the peak load stated by FMVSS214 side impact safety standard (300mm max. allowable inward deformation/ intrusion level) the equivalent IM7-carbon-epoxy composite beam

thickness about 4.32mm, so that the laminate thickness was calculated as follows:

Lamina thickness = number of orientation * fiber thickness + epoxy thickness

Lamina thickness = 4(0.0052mm) + 0.33mm

Lamina thickness = 0.358mm

Therefore, based on fiber volume fraction the numbers of layers (laminas) (N) can be:

Proposed thickness of anti-intrusion beam and pillars = N (fiber thickness + epoxy thickness)

Number of layers (N) = 4.32mm/0.36mm

Number of layers (N) = 12 layers

Orientation of ply is one of the fundamental advantages of laminates is the ability to adapt and control the fiber orientation for better material property. It is therefore important to know how the plies contribute to the laminate resistance, taking into account their relative orientation with respect to the loading direction. The car side-body structure the paper has considered a symmetric and balanced fiber orientation for better strength. Because any direction in the side-body structure has the probability to receive a crash during car collision, hence the system arrangement of fiber direction must be at same symmetric planes. Compatible to this fiber direction system is symmetry or angle ply arrangement which accepted by its

maximum stress value (0/45/90/-45) or ([0/+45/90]) 3s symmetry or angle ply laminates. Simulation Composite Design computes a set of 2-D and 3-D engineering properties for a homogeneous material that has the same effective properties as the laminate. For each ply in a laminate, Simulation Composite Design computes the plane stress (or reduced) stiffness matrix [Q] expressed in the global coordinate system (see appendices). Once the [Q] matrix is computed for a particular ply, the global stress components {σ_x} in the ply can be computed by multiplying the [Q] matrix by the global strain components {ε} in the ply, i.e.,

$$\{\sigma\} = [Q]\{\epsilon\}.$$

The Laminate Loads in this work is used to define the in-plane mechanical loads (i.e., the Axial Load, the Transverse Load, and the Shear Load) and bending loads that has been applied to the laminate to analyses the response of the material. The applications of this load either in global or local systems on the laminate which is used to compute the stress and strain in each ply of the laminate when the laminate is subjected to a specified set of in-plane and bending loads in either the global coordinate system or the principal material coordinate system of each individual ply.

Global stress –strain characteristics for each ply of IM7-Carbon/epoxy laminate, at Vf 60% is given in Table-2.

Table-2: Global stress–strain characteristics for each ply of IM7-Carbon/epoxy laminate, at Vf 60%¹⁴.

Ply	Longitudinal stress σ _x (MPa)	Longitudinal strain ε _x (mm/mm)	Transverse stress σ _y (MPa)	Transverse strain ε _y (mm/mm)	Shear stress G _{XY} (MPa)	Shear strain ε _{xy} (mm/mm)
1	1.85E+04	1.12E-01	-5.53E+01	-3.65E-02	1.98E+01	3.54E-03
2	4.57E+03	1.15E-01	2.88E+03	-3.55E-02	3.31E+03	4.06E-03
3	9.35E+02	1.18E-01	-5.47E+03	-3.45E-02	2.57E+01	4.59E-03
4	4.60E+03	1.21E-01	2.87E+03	-3.35E-02	-3.24E+03	5.11E-03
5	2.06E+04	1.24E-01	8.73E+00	-3.25E-02	3.16E+01	5.64E-03
6	5.44E+03	1.27E-01	3.67E+03	-3.14E-02	4.05E+03	6.17E-03
7	5.66E+03	1.31E-01	3.86E+03	-3.04E-02	4.24E+03	6.69E-03
8	2.22E+04	1.34E-01	5.67E+01	-2.94E-02	4.04E+01	7.22E-03
9	5.49E+03	1.37E-01	3.64E+03	-2.84E-02	-3.95E+03	7.74E-03
10	1.14E+03	1.40E-01	-4.23E+03	-2.74E-02	4.63E+01	8.27E-03
11	6.54E+03	1.43E-01	4.64E+03	-2.64E-02	4.98E+03	8.79E-03
12	2.43E+04	1.46E-01	1.21E+02	-2.53E-02	5.21E+01	9.32E-03

From Table-2 the following results are observed: i. Longitudinal stress σ_x (MPa) column ply # 3, and #10 has small stress value, therefore they fail to withstand for larger load. ii. In Transverse stress σ_y (MPa) column ply # 1, # 5, #8 and #12 has very small transverse stress value, therefore they fail to withstand for larger normal loads. iii. Shear stress G_{xy} (MPa) column ply # 1,#3,#5, #8 and #10 has very small transverse stress value, therefore they fail to withstand for larger shear loads.

The Laminate Mid-Plane Strain/Curvatures feature is used to compute the membrane strains and bending curvatures of the laminate's mid-plane that are caused by a specified set of in-plane loads and bending loads. Plane strains and curvatures of IM7 Carbon-epoxy laminate and 1025 Steel is listed in Table-3.

Table-3: Plane strains and curvatures of IM7 Carbon-epoxy laminate and 1025 Steel¹⁴.

Mid Plane Strains	IM7 Carbon-epoxy	Mild Steel
Longitudinal strain (ϵ_x) (mm/mm)	3.46E-02	2.73971E-03
Transverse strain (ϵ_y) (mm/mm)	1.03740E-02	1.20547E-02
Shear strain (ϵ_{xy}) (mm/mm)	1.03506E-02	2.45246E-03
Mid Plane Curvatures		
Longitudinal bending curvature K_x (1/mm)	9.50E-03	2.33533E-04
Transverse bending curvature K_y (1/mm)	4.61E-03	1.32130E-04
In-plane bending curvature K_{xy} (1/mm)	1.18E-02	5.67071E-04

Failure Criteria for Composite Materials at laminate level:

Base on the maximum stress failure criterion the failed first ply can be stated: A fiber-reinforced composite material in a general state of stress will fail when: Either, the maximum stress in the fiber direction equals the maximum stress in a uni-axial specimen of the same material loaded in the fiber direction when it fails; or, the maximum stress perpendicular to the fiber direction equals the maximum stress in a uni-axial specimen of the same material loaded perpendicular to the fiber direction when it fails; or, the maximum shear stress in the 1-2 planes equals the maximum shear stress in a specimen of the same material loaded in shear in the 1-2 planes when it fails. See tables in the appendix B.A simpler way to look at the maximum stress failure criterion is that material will not fail as long as

$$\left. \begin{aligned} \sigma_1^C < \sigma_1 < \sigma_1^T \\ \sigma_2^C < \sigma_2 < \sigma_2^T \\ |\tau_{12}| < \tau_{12}^F \end{aligned} \right\}$$

The Max Stress Criterion identifies three possible modes of failure: Longitudinal Failure, Transverse Failure, or Shear Failure. i. $\sigma_1T \equiv$ Value of σ_{11} at longitudinal tensile failure, ii. $\sigma_1C \equiv$ Value of σ_{11} at longitudinal compressive failure, iii. $\sigma_2T \equiv$ Value of σ_{22} at transverse tensile failure, iv. $\sigma_2C \equiv$ Value of σ_{22} at transverse compressive failure, v. $\tau_{12} \equiv$ Absolute value of σ_{12} at longitudinal shear failure, vi. Longitudinal Failure occurs whenever $\sigma_{11} \geq \sigma_{1T}$ or $\sigma_{11} \leq \sigma_{1C}$, vii. Transverse Failure occurs whenever $\sigma_{22} \geq \sigma_{2T}$ or $\sigma_{22} \leq \sigma_{2C}$, viii. Longitudinal Shear Failure occurs whenever $|\sigma_{12}| \geq |\sigma_{\max 12}|$, ix. Failure Index = Max. Absolute Value of ($\sigma_{11} / \sigma_{1T}$, $\sigma_{11} / \sigma_{1C}$, $\sigma_{22} / \sigma_{2T}$, $\sigma_{22} / \sigma_{2C}$, σ_{12} / τ_{12}).

Since the failure index is a simple ratio of stresses, the failure load can be computed by simply dividing the applied load by the failure index. For example, consider a composite material that is subjected to a transverse normal stress of 1 psi. If the computed failure index is 0.0002, then the transverse normal stress at failure is (1 psi)/0.0002 = 5000 psi. The simulated result on failure modes for IM7 Carbon/epoxy laminate is given in Table-4.

Table-4: Simulation result of first ply failure based on max stress criteria.

First Ply Failure			
Material	Ply No	Failure Index	Safety Factor
IM7-Carbon/Epoxy	Longitudinal Failure in Ply: 1	2.29463 E+04	4.35801 E-05
Mild Steel	Longitudinal Failure in Ply: 1	1.00430 E+01	9.95723 E-02

Simulation result of first ply failure stresses survey based on max stress criteria is listed in Table-5.

Table-5: Simulation result of first ply failure stresses survey based on max stress criteria.

+X-Direction	Transverse Failure in Ply:12	4.11300E+02 (MPa)
-X-Direction	Longitudinal Failure in Ply: 10	-4.79700E+02 (MPa)
+Y-Direction	Transverse Failure in Ply: 1	4.11300E+02 (MPa)
-Y-Direction	Longitudinal Failure in Ply: 3	-4.79700E+02 (MPa)
XY-Direction	Shear Failure in Ply: 1	3.71700E+02 (MPa)

Using the laminate survey utility the strength of laminate simulated to predicted how the laminate properties will vary with different laminate layups and we can predict the laminate global properties: Laminate material stiffness (E_x , E_y , G_{xy} , NU_{xy}), Longitudinal Tensile Strength σ_{1t} , Longitudinal Compressive Strength σ_{1c} , Transverse Tensile strength σ_{2t} , Transverse Compressive Strength σ_{2c} , and In-plane shear

Strength σ_{12} with defined layup angles. The failure load directions in the laminate is graphically shown in figure 3. Most of the car body panels constructed from structural plate or shell element in to different shapes and sizes. The thickness restriction ($h \ll W, h \ll L$) is necessary to ensure that practical methods of loading the plate primarily results in in-plane deformation and bending deformation. In other words, the plate does not exhibit significant transverse shear deformation or transverse normal deformation ($\epsilon_{xz} \approx 0, \epsilon_{yz} \approx 0, \epsilon_{zz} \approx 0$). Under these conditions, "Classical Lamination Theory" is appropriate for modeling the response of the plate to in-plane loads and bending loads, or modeling the lower natural vibration frequencies of the plate and the buckling loads of the plate. Such structures are agreeable to the assumption that the bending strains vary linearly through their thickness and any in-plane (membrane) loading leads to strains which are constant through the thickness. The shell or plate bending element, therefore, has a readymade strain field assumption through the thickness so that we only need to describe variations over the plate or shell mid-surface.

Results and discussion

Bending load on steel plate and Carbon/Epoxy shell with the indicated boundary conditions simulated result is given in Table-6. The laminated plate stability analysis feature allows the user to compute and predict the critical buckling load of a laminated plate subjected to uni-axial in-plane compression or biaxial in-plane compression. This is very important parameter for real life car body structure. Buckling/compression load on steel plate and Carbon/Epoxy shell with the indicated boundary conditions simulated result is given in Table-7.

Finite Element analysis of Composite Laminate: SHELL181 is suitable for analyzing thin to moderately-thick shell structures. It is a four-node element with six degrees of freedom at each node: translations in the x, y, and z directions,

and rotations about the x, y, and z-axes. (If the membrane option is used, the element has translational degrees of freedom only). The degenerate triangular option should only be used as filler elements in mesh generation. SHELL181 is well-suited for linear, large rotation, and/or large strain nonlinear applications. Change in shell thickness is accounted for in nonlinear analyses. In the element domain, both full and reduced integration schemes are supported.

The material typical selected for the study was " *STRUCTURAL* LINEAR, *ELASTIC *ISOTROPIC* for steel & *ORTHOTROPIC* for Carbon/Epoxy composite". The model permits the description of a single ply of an Isotropic steel shell /lamina and orthotropic composite laminate material using the following elastic material constants E1, E2, G12, G13, and G23. The alignment of the fiber track for each composite material ply can be defined autonomously. The ANSYS Mechanical ADL *ORIENTATION card was used to, with the application of local or the global coordinate system. In the case of flat plate study, all materials are oriented with global coordinate system relatively. It includes the *INTEGRATION PTS = 3*, which locates an integration point at the top, middle, and bottom of each layer. Since for solving a linear problem, 3-integration points will give us more accuracy to solve the problem. The plate geometry has defined the same in-plane dimensions (width = 500 mm and length=1000 mm) of steel plate with 2.00 mm thickness and the laminated late with 4.32 mm thick. Geometry and Symmetrical Boundary Conditions and Mesh Refinement of plate is illustrated in Figure-4.

ANSYS analysis for bending, buckling loads: The following assumptions are made in the classical lamination theory to develop the relationships: i. Each lamina is orthotropic. ii. Each lamina is homogeneous. iii. A line straight and perpendicular to the middle surface remains straight and perpendicular to the middle surface during deformation.

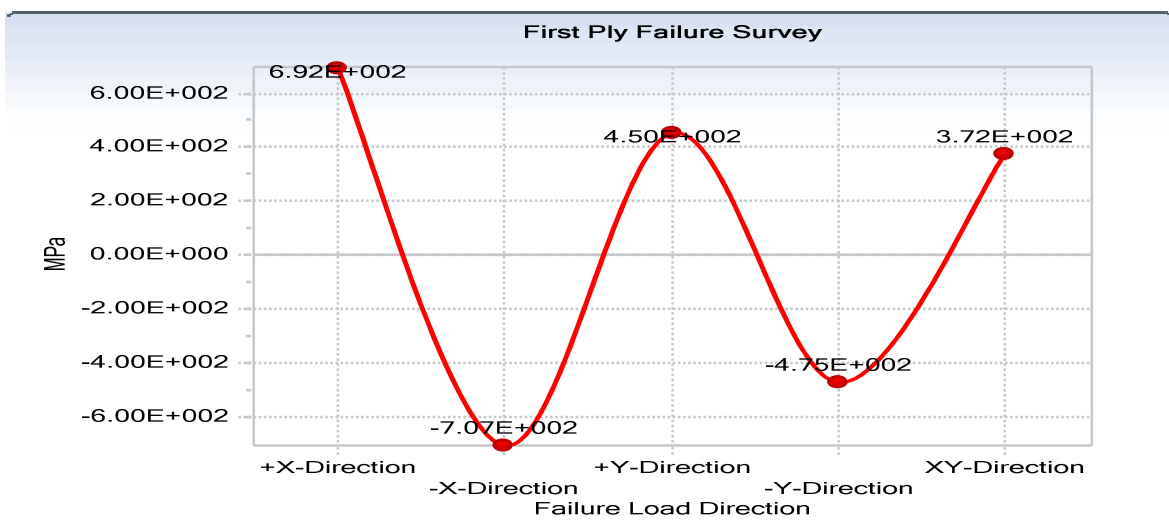


Figure-3: The failure load directions in the laminate.

Table-6: Bending load on steel plate and Carbon/Epoxy shell with the indicated boundary conditions simulated result.

Bending load conditions	Extent of loads [MPa]/N	Boundary conditions	Transverse deflection of Steel(mm)	Transverse deflection of Carbon/Epoxy(mm)
Uniformly distributed transverse load	1000	Simply supported at 4-corners	2.18209E+06	1.75445E+06
	5000	“	1.09104E+07	8.77227E+06
	8000	“	1.74567E+07	1.40356E+07
	10000	“	2.18209E+07	1.75445E+07
Uniformly distributed transverse load	1000	Clamped at 4-corners of plate	6.11375E+05	4.87872E+05
	5000	“	3.05688E+06	2.43936E+06
	8000	“	4.89100E+06	3.90298E+06
	10000	“	6.11375E+06	4.87872E+06
Concentrated load[N]	1000	Simply supported at 4-corners	1.40871E+01	1.06889E+01
	5000	“	7.04357E+01	5.34443E+01
	8000	“	1.12697E+02	8.55108E+01
	10000	“	1.40871E+02	1.06889E+02

Table-7: Buckling /compression load on steel plate and Carbon/Epoxy shell with the indicated boundary conditions simulated result.

Buckling load conditions	Boundary conditions	Critical buckling load Steel plate	Critical buckling load carbon/epoxy laminate or plate
Uni-axial uniformly distributed compression (buckling) load[N/mm]	Simply supported at 4-corners	7.15885E+01	9.00826E+01
Uni-axial uniformly distributed compression (buckling) load[N/mm]	Clamped at 4-corners of plate	7.93412E+01	1.23180E+02
Biaxial uniformly distributed compression (buckling) load	Simply supported at 4-corners	1.43177E+01	1.80165E+01

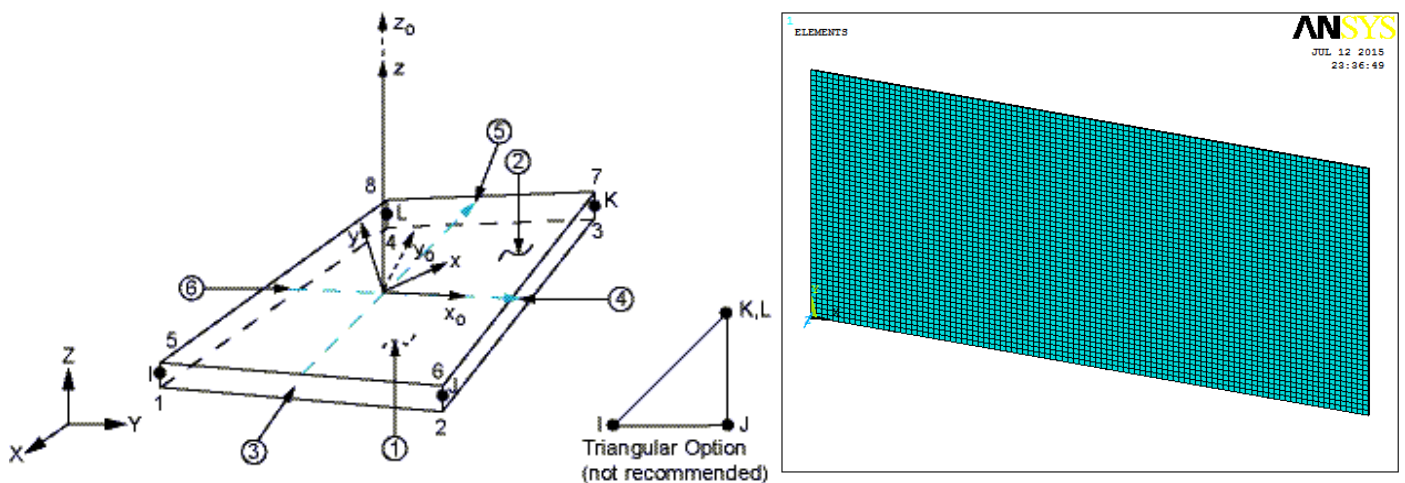


Figure-4: Geometry and Symmetrical Boundary Conditions and Mesh Refinement of plate.

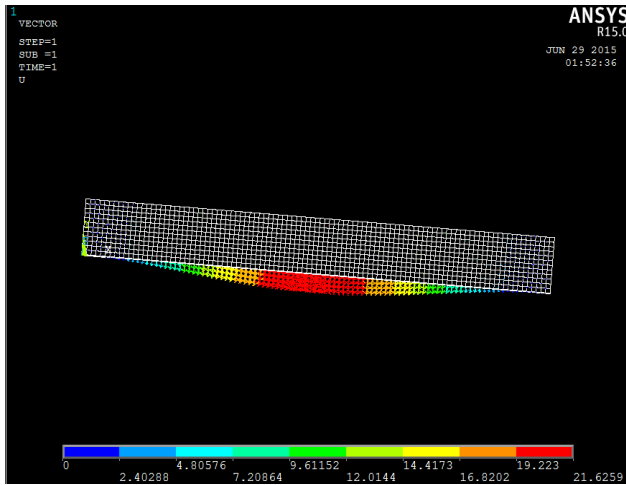
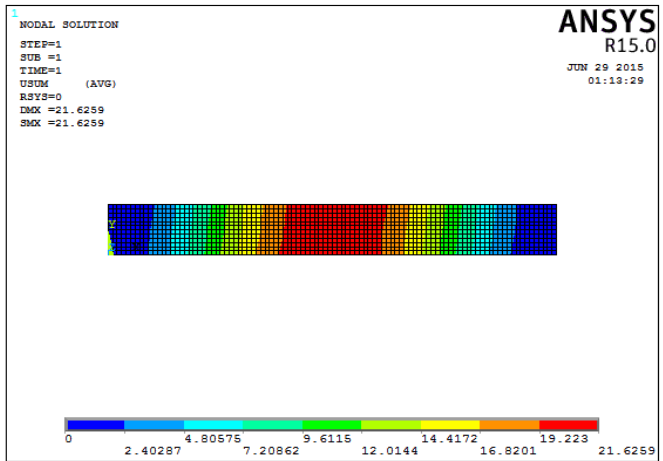


Figure-5: Displacement of the composite plate in the Z-Direction Due to $F_z=-1\text{KN}$.



The ansys result shows the displcement to the direction of applied bending load on the plate in Figure-5. The deflection of the plate at both ends is zero as it constrained at two ends and gradually increased to the point of load application where the maximum deflection is observed.

to the ends of the plate where the minimum transverse stress is observed. So that it is the converse to the in-plane stress distribution in x-direction.

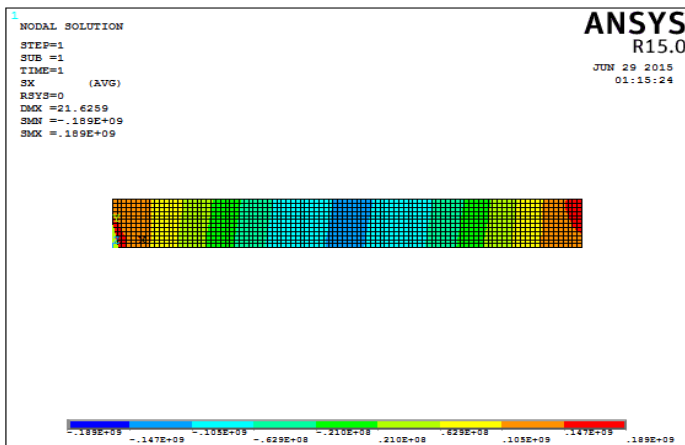


Figure-6: Stress distribution (sx) in ANSYS for a $[0/+45/90]_s$ Laminate ($F_z=-1\text{KN}$).

In Figure-6 shows mid plane the longitudinal stress distribution for the applied bending transverse load. Thus the longitudinal stress minimum value at the point where the load applied on the laminate and increased to the ends of the plate where the maximum longitudinal stress happened due to high tension with fixed boundary conditions.

From the Figure-7 it can be determined that the response of the materials against the bending load $F_z=1\text{KN}$. Thus ANSYS simulated result indicates that, the maximum strain in the x-direction is located in the mid plane at the fixed ends points.

The out-of-plane stress and strain distribution shown in Figure-8 and Figure-9 shows the interaction of the layers well. The magnitude of the out-of-plane of mid plane stress is higher at the point where the load applied on the laminate and decreased

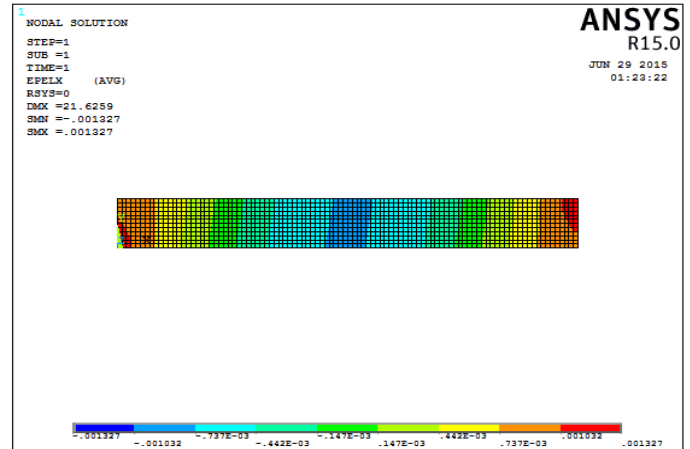


Figure-7: Strain distribution (ϵ_x) in ANSYS for a $[0/+45/90]_s$ Laminate ($F_z=1\text{KN}$).

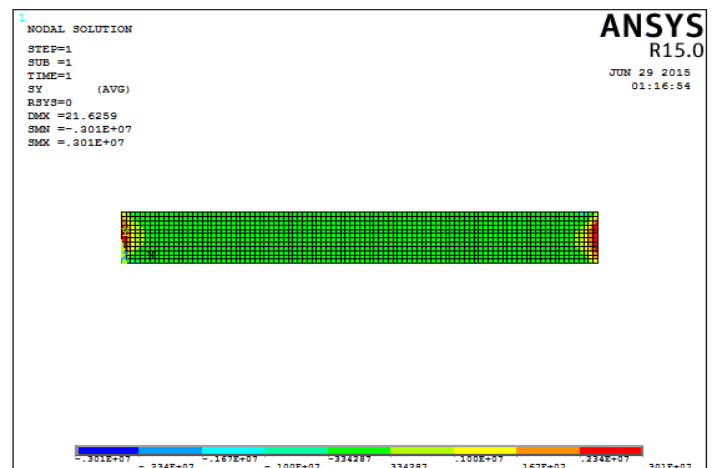


Figure-8: Stress distribution (sy) in ANSYS for a $[0/+45/90]_s$ Laminate ($F_z=1\text{KN}$).

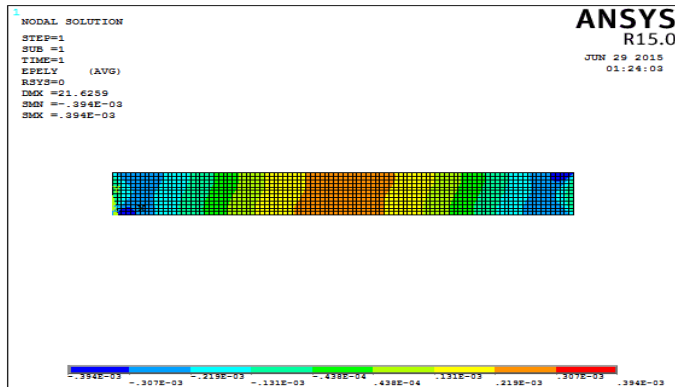


Figure-9: Strain distribution (ϵ_y) in ANSYS for a [0/+45/90]_s Laminate($F_z=1\text{KN}$).

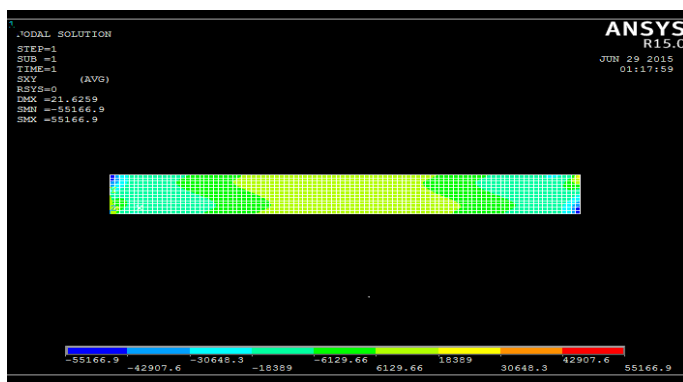


Figure-10: Shear Stress distribution (S_{xy}) in ANSYS for a [0/+45/90]_s Laminate($F_z = -1\text{KN}$).

The Figure-10 shows the inter-laminar /shear stress distribution. The magnitude of the inter-laminar /shear stress of mid plane stress is higher at the point where the load applied on the laminate and decreased to the ends of the plate where the minimum inter-laminar /shear stress is observed. In tensile failure model with the addition of failure test, modification has done in the basic orthotropic linear elastic tensile behavior of the standard ANSYS composite material. Because of the two reasons initiate breakages in fiber structure i.e. One is linear elastic behavior and another is catastrophic failure. To simulate this, a maximum stress principle is applied in the fiber track, which when exceeded results in a decrease of the Young's modulus in both the X and Y direction to a minimal value of 1575 MPa and the decrease of Poisson's Ratio to 0.27. This denotes the loss of local tensile load carrying ability in both orders when fiber failure arises in a composite ply.

Failure identified if: $\sigma_{11T} > \sigma_{1uT}$

Failure identified if: $\sigma_{22T} > \sigma_{2uT}$.

ANSYS simulated result in for the plate due to bending load 1KN is 189MPa and ultimate longitudinal tensile strength of Carbon/Epoxy composite is 1575 MPa for X-direction. ANSYS simulated result in transverse direction for the plate due to bending load 1KN is 189MPa and ultimate transverse tensile

strength of Carbon/Epoxy composite is 954 MPa. Therefore, the ANSYS simulated result shows that the plate has not failed for the bending load with the given boundary.

Section properties for car side-boy structures: The most common Crosssection currently used in most car body structures are channels, plates and C/I/T/Hat sections. However, in this paper some optimizations on the sections like box /circular tube & hat have examined using finite element methods. Cases were considered to examine the section properties for side impact beam and pillar or rail boy structures. The first case is side impact beam for the door and the second case for pillars for both materials aforementioned above and the dimensions of these structures was taken from Liffan car indicated in chapter three. The results were compared to show the response of sections for the defined apply loads like bending, torsion and buckling in different loading conditions as well as fixed-ends boundary conditions.

Finite element solution side impact beam case: The beam bending feature allows the user to perform a structural analysis (calculate deflections, reaction forces, moments, bending/shear stresses, etc.) of a tube/beam in bending using beam theory calculations. Loading applications is uniform distributed loads, with fixed end boundary conditions. Bending load on steel side impact beam and Carbon/Epoxy shell with the indicated boundary conditions simulated result is given in Table-8.

The torsion feature allows the user to perform a structural analysis (calculate tensional stiffness, angle of twist, shear stresses, etc.) of a tube/beam in torsion using analytical algorithms which is given in Table-9.

The column stability feature allows the user to perform a stability analysis (calculate critical loads and stress) of a column. Loading applications is uniform distributed loads, with fixed end boundary conditions. Buckling /compression load on steel side impact beam and Carbon/Epoxy shell with the indicated boundary conditions simulated result is listed in Table-10.

The column stability feature allows the user to perform a stability analysis (calculate critical loads and stress) of a column. Loading applications is uniform distributed loads, with fixed end boundary conditions. The Stress-Strain and Strength analysis the Autodesk simulation composite design simulated Global/Local Stress/Strain, Mid-Plane Strains/Curvatures, First Ply Failure and Progressive Failure value of IM-Carbon/Epoxy laminate level have been determined. We have been concluding the response of Carbon/Epoxy composite laminate shows better result than ordinary steel. Based on "Classical Laminate Theory", we have been modelling the response of the plate to in-plane loads and bending loads, or the buckling loads of the plate. Therefore, we have conclude the result: From the table 6 the response of the plate for different bending load and boundary conditions, the result indicates the transverse

deflection of Carbon/Epoxy (mm) plate is 19.6% lesser than the steel one. And from the Table-10 the stability of the plate for uni and bi-axial uniformly distributed compression (buckling) load[N/mm] with different boundary conditions, the result indicates Critical buckling load carbon/epoxy laminate or plate is 20.5% ,44% and four folds larger than the steel plate respectively. Finite element method using ANSYS simulated result shows that the Carbon/Epoxy composite plate has not

failed for the tensile, compressive and inter-laminar shear failures mode under the applied bending load with the given boundary conditions. The results were compared in the above tables (Table 4 –to-10) to show the response of sections for the defined apply loads like bending, torsion and buckling in different loading conditions as well as fixed-ends boundary conditions.

Table-8: Bending load on steel side impact beam and Carbon/Epoxy shell with the indicated boundary conditions simulated result.

Secti ons	Bending loads	Boundary condition s	Max. Moment um (N- mm)at x(mm)st eel	Max. Moment um (N- mm)at x(mm) carbon/e poxy	σ max. Induced by M max. (Mpa) steel	σ max. Induced by M max. (Mpa) carbon/e poxy	Max. shear stress (Mpa) steel	Max. shear stress (Mpa) carbon/e poxy	δ Max. deflec tion (mm) at x (mm) steel	δ Max. deflecti on (mm) at x (mm) carbon/ epoxy
	Distributed 1.00000E+03	fixed both ends	3.37500 E+07	3.38E+7	8.25603 E+03	3.58E+3	1.26404 E+03	5.56E+2	123	127
	Distributed1.000 00E+03	fixed both ends	3.37500 E+07	3.38E+7	1.11653 E+04	4.70E+3	1.16129 E+03	6.02E+2	165.6 6	177.7
	Distributed1.000 00E+03	fixed both ends	3.37500 E+07	3.38E+7	2.22070 E+04	9.34E+3	2.23812 E+03	9.66 E+2	330.7 4	332

Table-9: Torsion load on steel side impact beam and Carbon/Epoxy shell with the indicated boundary conditions simulated result,

Secti ons	Torsion loads	Boundary condition s	Tension al stiffness steel(M pa)	Tensional stiffness carbon/epox y(Mpa)	Averag e shear stresses steel(M pa)	Average shear stress carbon/epox y(Mpa)	Max Warpi ng Rigidit y Shear Stress steel(Mpa)	Max Warping Rigidity Shear Stress carbon/epox y(Mpa)	Amount of twist over the defined length steel	Amount of twist over the defined length carbon/ epoxy
	1.00000 E+03	fixed both ends	1.13405 E+10	8.83E+9	1.37061 E-01	5.68E-2	-	-	4.54709 E-03	5.84E- 3
	1.00000 E+03	fixed both ends	3.13482 E+07	1.07E+8	9.58620 E-02	8.50E-2	1.1368 3E-01	-1.12E-1	6.04892 E-01	2.76E- 1
	1.00000 E+03	fixed both ends	3.91899 E+09	3.22E+9	3.28992 E-01	1.387E-1	-	-	1.31580 E-02	1.603E -2

Table-10: Buckling /compression load on steel side impact beam and Carbon/Epoxy shell with the indicated boundary conditions simulated result.

Sections	Buckling loads	Boundary conditions	Critical Load steel(N)	Critical Stress Steel(MPa)	Critical Load carbon/epoxy (N)	Critical Stress carbon/epoxy(MPa)
	1.00000E+03	fixed both ends	1.26983E+06	3.56693E+03	1.23E+6	1.52E+3
	1.00000E+03	fixed both ends	9.42522E+05	3.04039E+03	8.79E+5	1.18E+3
	1.00000E+03	fixed both ends	4.72091E+05	2.34799E+03	4.69E+5	1.00E+3

Conclusion

i. The weight reduction of side impact beam in the study is 65%,
 ii. Carbon/epoxy composite door side impact beam is more effective for side impact protection standards. iii. Although the Carbon/epoxy composite side body structures fail by buckling during impact loading, buckling failure can be reduced by using proper design, fiber orientation, fiber matrix combination and geometric optimization of cross sections. iv. Changes in the fiber orientation and fiber matrix volume ratio causes the optimization of the mechanical properties.

References

- Cramer D.R., Taggart D.F. and Inc H. (2002). Design and manufacture of an affordable advanced-composite automotive body structure. *In Proceedings from The 19th international battery, hybrid and fuel cell electric vehicle symposium and exhibition*, 1-12.
- Miravete A., Castejon L., Bielsa J. and Bernal E. (2003). Analysis and prediction of large composite structures: three case studies. *Proc. of Composite, Zaragoza University, Spain*.
- Melvin J.W., Begeman P.C. and Foster C.D. (2002). Sled Test Evaluation of Racecar Head/Neck Restraints Revisited. SAE No: 2004-01-3516
- Park C.K., Kan C.D., Reagan S., Deshpande B. and Mohan P. (2012). Crashworthiness and numerical analysis of composite inserts in vehicle structure. *SAE International Journal of Passenger Cars-Mechanical Systems*, 5(2012-01-0049), 727-736.
- Farley G.L. and Jones R.M. (1992). Crushing characteristics of continuous fiber-reinforced composite tubes. *Journal of composite Materials*, 26(1), 37-50.
- Gamble K., Pilling M. and Wilson A. (1995). An automated finite element analysis of the initiation and growth of damage in carbonfibre composite materials. *Composite structures*, 32(1-4), 265-274.
- Bames G., Coles I., Roberts R., Adams D.O. and Gamer Jr, D.M. (2010). Crash safety assurance strategies for future plastic and composite intensive vehicles (PCIVs) (No. DOT-VNTSC-NHTSA-10-01). United States. National Highway Traffic Safety Administration.
- Honnagangaiah K. (2006). Design and Evaluation of Car Front Sub frame Rails in a Sedan and its Corresponding Crash Injury Response. M.S. Thesis, Department of Mechanical Engineering, Wichita state university.
- Thornton P.H. and Jeryan R.A. (1988). Crash Energy Management in Composite Automotive Structures. *International Journal of Impact Engineering*, 7(2), 167-180.
- Thornton P.H. and Edwards P.J. (1982). Energy Absorption in Composite Tubes. *Journal of Composite Materials*, 16(6), 521-545.
- Nee A.Y. (Ed.). (2015). Handbook of manufacturing engineering and technology. Springer Reference.
- Mandell S.P., Kaufman R., Mack C.D. and Bulger E.M. (2010). Mortality and injury patterns associated with roof crush in rollover crashes. *Accident Analysis & Prevention*, 42(4), 1326-1331.
- Capelaa C., Oliveiraa S.E., Pestanaa J. and Ferreiraa J.A.M. (2017). Effect of Fiber length on Mechanical Properties of high dosage Carbon reinforced. *Procedia Structural Integrity*, 5, 539-546.
- Budiansky B. and Fleck N.A. (1993). Compressive failure of fibre composites. *Journal of the Mechanics and Physics of Solids*, 41, 183-211.